

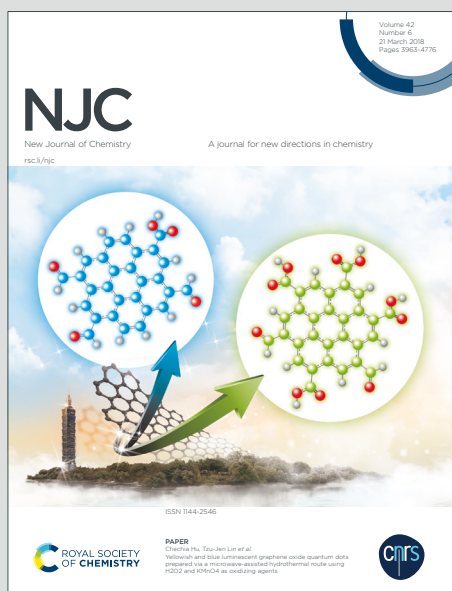
NJC

New Journal of Chemistry

Accepted Manuscript

A journal for new directions in chemistry

This article can be cited before page numbers have been issued, to do this please use: C. Caltagirone, V. Lippolis, M. E. Olmos, L. Coconubo, S. Moreno, G. Picci, M. Monge and J. M. López-de-Luzuriaga, *New J. Chem.*, 2026, DOI: 10.1039/D6NJ00558F.



This is an Accepted Manuscript, which has been through the Royal Society of Chemistry peer review process and has been accepted for publication.

Accepted Manuscripts are published online shortly after acceptance, before technical editing, formatting and proof reading. Using this free service, authors can make their results available to the community, in citable form, before we publish the edited article. We will replace this Accepted Manuscript with the edited and formatted Advance Article as soon as it is available.

You can find more information about Accepted Manuscripts in the [Information for Authors](#).

Please note that technical editing may introduce minor changes to the text and/or graphics, which may alter content. The journal's standard [Terms & Conditions](#) and the [Ethical guidelines](#) still apply. In no event shall the Royal Society of Chemistry be held responsible for any errors or omissions in this Accepted Manuscript or any consequences arising from the use of any information it contains.

ARTICLE

Structural and computational evidence of rare synergic N(amide)H...Au(I) and N(amidate)...Au(I) secondary bonding interactions

Received 00th January 20xx,
Accepted 00th January 20xx

DOI: 10.1039/x0xx00000x

Laura Coconubo-Guio,^a Sonia Moreno,^a Giacomo Picci,^b Miguel Monge,^a José M. López-de-Luzuriaga,^a M. Elena Olmos,^{*a} Claudia Caltagirone,^{*b} Vito Lippolis^{*b}

This work focusses on weak NH...Au(I) non-covalent interactions (NCIs), a subject of ongoing debate. It reports the synthesis and characterization of new gold(I) complexes featuring the pincer ligand N,N'-bis{(2-diphenylphosphanyl)phenyl}-2,6-pyridinedicarboxamide (**L**). Rare examples of N(amide)H...Au(I) interactions in different coordination environments are examined. In the neutral complex [Au(L-*H*)] (**3**), both a directional N(amide)H...Au(I) contact consistent with a metal-centered hydrogen bond, and an uncommon secondary N(amidate)...Au interaction are identified, highlighting their relevance for future structural and computational analyses.

Introduction

Non-covalent interactions (NCIs), including hydrogen,¹ halogen² and chalcogen bonding,³ play an essential role in supramolecular and coordination chemistry, where they govern key concepts such as preorganization, complementarity, cooperativity, selectivity and discrimination.⁴ Their ability to influence structure, stability and reactivity has made them powerful tools for rational molecular design across fields ranging from crystal engineering to catalysis. Recent literature continues to emphasise the centrality of NCIs in dictating the behaviour of coordination compounds and the diversity of weak bonding patterns accessible to transition metals.⁵ Such studies highlight the need for deeper understanding of special bonding motifs already known in coordination chemistry and their structural and functional consequences.

Within this broad context, weak interactions of the type M...H-X (X = C, N, O, halogens) involving electron-rich transition metals have attracted increasing interest. These contacts, frequently interpreted as metal-centred hydrogen bonds,⁶⁻⁸ are relevant to fundamental processes such as the protonation of transition metals to form metal hydrides, and to X-H activation in catalysis. Their identification, however, is complicated by the coexistence of multiple NCIs, geometric constraints and metal-dependent electronic effects.

Gold(I) provides a particularly compelling platform for investigating such interactions. Its closed-shell d¹⁰ configuration,

strong relativistic effects, high electronegativity and preference for linear coordination endow gold(I) compounds with a remarkable efficiency in both heterogeneous and homogeneous catalysis,⁹⁻¹¹ and enable unconventional secondary-bonding. Despite possessing characteristics that should favour X-H...Au(I) hydrogen bonding, the capacity of gold(I) to function as a true hydrogen-bond acceptor remains a subject of ongoing debate.¹²⁻¹⁸ Distinguishing authentic Au...H hydrogen bonds from short contacts constrained by packing forces, competing NCIs, including metallophilic interactions, or the ligand framework is particularly challenging.^{12,19} Spectroscopic signatures typical of hydrogen bonding are often ambiguous in gold complexes due to the relativistic and electronic environment at the metal centre, further complicating reliable identification.^{20,21} Consequently, only limited well-supported examples exist, underscoring the need for new systems that expand the structural diversity available for analysis.

Advancing this field requires systematic exploration of gold(I) complexes capable of supporting putative X-H...Au(I) interactions, allowing identification of consistent geometric or electronic trends that clarify their origin and significance. Recent contributions show that *ortho*-aminophenylphosphines constitute promising scaffolds for probing such weak interactions, as they combine strong electron-donating phosphorus donors with strategically positioned N-H groups oriented toward the metal centre.^{21,22} These ligand platforms offer an opportunity to examine how coordination environment and ligand flexibility influence the emergence of weak, metal-centred NCIs.

Herein, we investigate the coordination chemistry of gold(I) with the flexible pincer ligand N,N'-bis{(2-diphenylphosphanyl)phenyl}-2,6-pyridinedicarboxamide (**L**) (Scheme 1), designed to probe N(amide)H...Au(I) interactions across distinct coordination environments. The conformational adaptability of **L** enables access to structural arrangements not

^a Departamento de Química, Instituto de Investigación en Química de la Universidad de La Rioja (IQUIR), Universidad de La Rioja, Complejo Científico Tecnológico, 26006-Logroño, Spain.

^b Dipartimento di Scienze Chimiche e Geologiche, Università degli Studi di Cagliari, S.S. 554 Bivio per Sestu, 09048 Monserrato (CA), Italy.

E-mails: m-elena.olmos@unirioja.es, lippolis@unica.it, caltagirone@unica.it

†Supplementary Information available: Mass spectra, IR spectra, NMR spectra, X-ray data, and computational data. See DOI: 10.1039/x0xx00000x

attainable with more rigid pincer frameworks, providing an ideal platform for identifying diverse weak interactions around gold. In this work, structural and computational analyses reveal rare examples of N(amide)H...Au(I) hydrogen-bond-like interactions together with an unusual secondary N(amidate)...Au(I) contact. These findings expand the limited catalogue of existing special bonding motifs in gold(I) coordination chemistry and provide new insights into the fundamental characteristics governing weak, metal-centred NClis.



Scheme 1. Molecular structure of *N,N'*-bis((2-diphenylphosphanyl)phenyl) 2,6-pyridinedicarboxamide (**L**).

Results and discussion

Synthesis and characterization.

The pincer ligand **L** was synthesised following the procedures reported by B. L. Feringa,²³ and Y. Liu,²⁴ by reacting 2,6-pyridinedicarbonyl dichloride with 2-(diphenylphosphino)aniline in a 1:2 molar ratio in THF under a nitrogen atmosphere (see Experimental Section). A slight excess of triethylamine was added to promote partial deprotonation of the aniline, thereby facilitating the formation of the amide groups.

Reaction of **L** with [AuCl(tht)] (tht = tetrahydrothiophene) in 1:2 and 1:1 molar ratio in CH₂Cl₂ afforded white solid powders corresponding to the formulation [(AuCl)₂(**L**)] (**1**) and [AuCl(**L**)] (**2**), respectively (see Figures S1 and S2 for mass spectra in the Electronic Supplementary Information, ESI). Both compounds are moderately stable to air and moisture at room temperature. They are soluble in organic solvents such as acetone and in chlorinated solvents such as CH₂Cl₂ and CHCl₃, but insoluble in *n*-hexane and diethyl ether. Molar conductivity measurements in acetone solutions (5 × 10⁻⁴ M) indicate that both behave as non-electrolytes, consistent with their neutral nature, showing values of 4.1 (**1**) and 3.2 (**2**) Ω⁻¹·cm²·mol⁻¹, respectively. The infrared spectra of **1** and **2** display bands corresponding to the stretching vibration of the amide group in the ranges 3017–2946 cm⁻¹ and 3201–3055 cm⁻¹, respectively (Figures S3 and S4), which are only slightly shifted with respect to the corresponding vibration in the free ligand (3338–3275 cm⁻¹)²⁴. This observation, together with the presence of a single, markedly low-field-shifted resonance in the ³¹P{¹H}-NMR spectrum (CDCl₃) of the two compounds [δ_P = 23.98 ppm for **1**, 34.97 ppm for **2**, -19.73 ppm for **L**²⁴] (Figures S5 and S6), and the slight displacement of the amidic proton signals in the ¹H-NMR spectra (CDCl₃) [δ_H = 9.36 ppm for **1**, 11.79 ppm for **2**, 10.58 ppm for **L**²⁴] (Figures S7 and S8), clearly indicates that ligand **L** coordinates to the metal center(s) through the phosphorus atoms rather than through the nitrogen ones. An X-ray

diffraction analysis was carried out to confirm the structure of **1** and **2** and establish the coordination mode of **L** to the gold(I) center(s).

Crystals of **1** and **2**·1.5CH₂Cl₂, suitable for X-ray diffraction analysis, were obtained by slow diffusion of *n*-hexane into a saturated CH₂Cl₂ solution of the respective white solid samples at room temperature.

Regarding the crystal structure of compound **1** (Figure 1, Tables 1 and 2), it features a gold(I) center coordinated to each phosphorous donor atom from ligand **L** [Au1–P1 = 2.2307(10) Å, Au2–P2 = 2.2266(11) Å], with a chloride ligand completing a linear coordination environment [Au1–Cl1 = 2.2718(11) Å, Au2–Cl2 = 2.2644(13) Å]. The polydentate ligand **L** thus acts as a bridge between the two metal centers. The molecule is not completely symmetrical, since one of the amide hydrogen atoms is involved in an intramolecular N–H...Au contact with one of the gold atoms [H1...Au1 = 2.977(48) Å, N1...Au1 = 3.5655(6) Å, N1–H1–Au1 = 146(5)°], whereas at the opposite end of the molecule the H3...Au2 distance of 3.44 Å, and especially the N–H...Au angle of 88°, suggest the absence of any N–H...Au interaction.

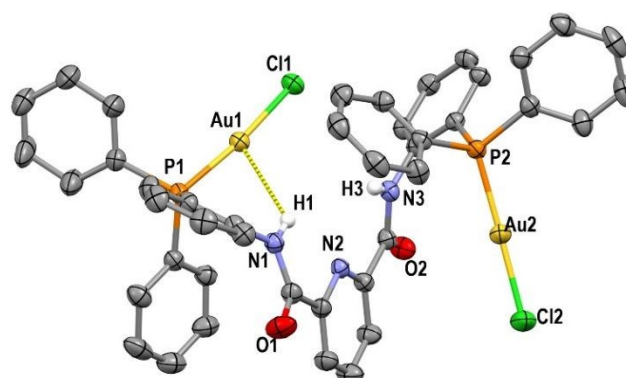


Figure 1. Molecular structure of **1** with the labelling scheme for the atom positions. Hydrogen atoms, except those of the NH groups, have been omitted for clarity.

This asymmetry is also reflected in the larger deviation from linearity at the gold(I) centre involved in the H...Au contact, where the P1–Au1–Cl1 angle is 173.10(4)°, compared to 176.15(6)° for the P2–Au2–Cl2 angle at the second metal centre. Neither intra- nor intermolecular Au...Au interactions are observed, while in the crystal packing, intermolecular C–H...O hydrogen bonds (Tables 2 and S1) between adjacent units of **1** determine the formation polymeric chains (Figure S13A), and additional C–H...Cl hydrogen bonds (Tables 2 and S1) that connect neighbouring chains result in the formation of a two-dimensional network (Figure S13B).

To the best of our knowledge, N(amide)–H...Au interactions have not so far been discussed in the literature. Furthermore, the experimental authentication of a genuine N–H...Au hydrogen bond (mainly involving amine groups) is a matter of ongoing debate.¹⁸ With the exception of very few examples of gold(I) compounds exhibiting in their crystal structure intermolecular H...Au distances significantly shorter (below 2.5 Å)^{13,18} than the sum of the corresponding van der Waals radii [$\Sigma_{vdw}(H, Au) = 2.86$ Å],²⁵ and N–H–Au angles markedly higher than 110°,^{13,18} whose bonding nature has



also been supported experimentally by spectroscopic evidence, the vast majority of reported cases claiming N-H...Au associations display H...Au separations close to the sum of the van der Waals radii (up to 3.0 Å) and N-H-Au angles in the range 100–130°, with a maximum at around 113°. Often, even when supported by computational studies, the presence of other concomitant non-covalent interactions involving the gold(I) centre and/or the NH group cast some doubts on the genuine role of these N-H...Au contacts within the coordination environment of the metal centre.

Table 1. Selected bond distances (Å) and angles (°) in the crystal structures of **1** and **2**·1.5CH₂Cl₂.

	1	2 ·1.5CH ₂ Cl ₂
Au–P	2.2307(10)	2.3179(11)
	2.2266(11)	2.3154(11)
Au–Cl/N	2.2718(11)	2.6424(12)
	2.2644(13)	
P–Au–Cl/N	173.10(4)	101.26(4)
	176.15(6)	102.38(4)
P–Au–P		156.23(4)

To obtain more conclusive structural evidence for the possible and uncommon¹³ N(amide)-H...Au interaction observed in compound **1**, we investigated compound **2**, prepared from the reaction of **L** with one equivalent of [AuCl(tht)], in which the coordination of both phosphine donors to the same gold(I) centre is expected.

In fact, in the crystal structure of **2**·1.5CH₂Cl₂ the gold(I) centre is tri-coordinated by two phosphorus atoms from ligand **L** [Au1–P1 = 2.3179(11) Å, Au1–P2 = 2.3154(11) Å] and one chloride ligand [Au1–Cl1 = 2.6424(12) Å], adopting a planar distorted T-shaped geometry (Figure 2a). These Au–P and Au–Cl bond lengths are markedly longer than those observed in **1**, as a consequence of the different coordination environment around the gold(I) centre. Furthermore, the P–Au–Cl angles of 101.26(4)° [P1–Au1–Cl1] and 102.38(4)° [P2–Au1–Cl1] are significantly smaller than the P1–Au1–P2 angle of 156.23(4)°, which lies halfway between those theoretically expected for trigonal-planar and linear coordination environments. This latter angle is much larger than that typically observed in gold(I) complexes featuring a coordination environment closer to trigonal planar and the same AuClP₂ fragment, in which longer Au–P and significantly shorter Au–Cl bond lengths are also generally recorded concurrently.^{26–30}

It is worth noting that, due to the chelating coordination of **L**, the hydrogen atoms of the amide groups are both brought in close proximity of the gold(I) centre, with H...Au distances of 2.8345(1) Å and 3.0316(1) Å for H1...Au1 and H3...Au1, respectively (see Tables 2 and S2). Both hydrogens also engage in hydrogen bonding with the chloride ligand, showing H...Cl distances of 2.635(2) Å (H1...Cl1) and 2.586(2) Å (H3...Cl1) (Tables 2 and S2). Compared to **2**·1.5CH₂Cl₂, in **1** the N(amide)-H...Au distance is intermediate between those found in **2**·1.5CH₂Cl₂, with H1...Au1 in the latter being slightly smaller than

the sum of the van der Waals radii, while the N1–H1–Au1 angle is wider in **1** than in **2**·1.5CH₂Cl₂.

As in the crystal structure of **1**, no Au...Au interactions are observed in the crystal packing of **2**·1.5CH₂Cl₂; however, intermolecular hydrogen bonds of different nature are present. Thus, bifurcated C–H...O contacts involving O2 (Tables 2 and S2) afford one-dimensional polymers that run parallel to the *b*-axis (Figure S14A) that are connected through C–H...O hydrogen bonds involving O1 (Tables 2 and S2), thus resulting in the formation of layers normal to the *c*-axis (Figure S14B and C). Finally, these planes are joint via C–H...Cl hydrogen bonds (Tables 2 and S2) that give rise to an extended 3D arrangement.

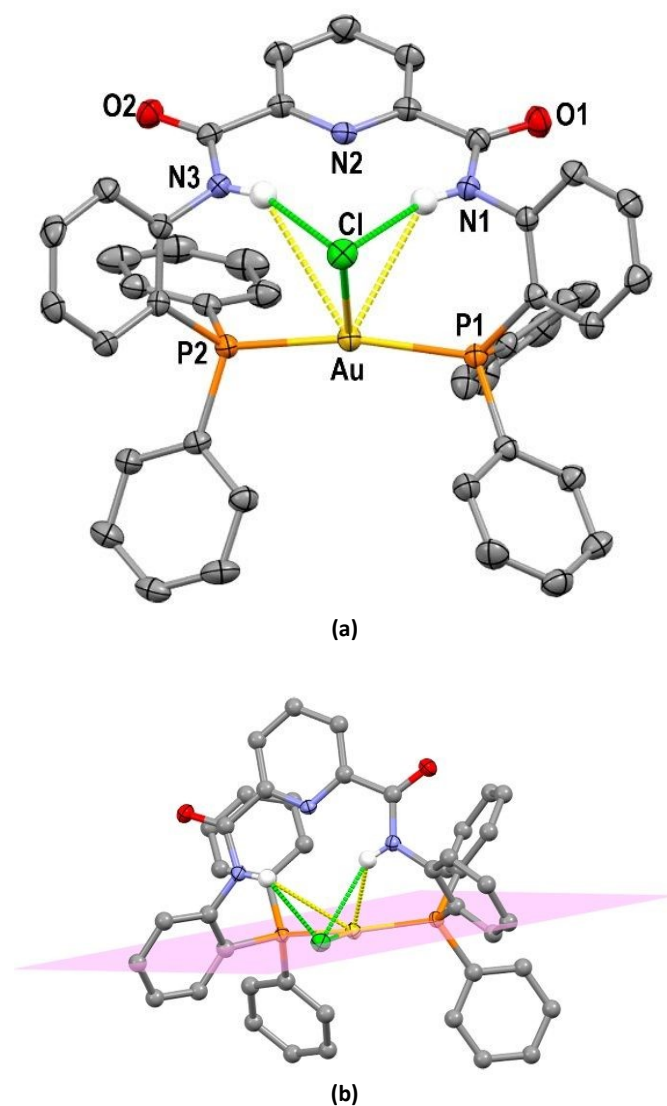


Figure 2. (a) Molecular structure of **2**·1.5CH₂Cl₂ with the labelling scheme for the atom positions (the crystallization solvent molecules and hydrogen atoms, except those of the NH groups, have been omitted for clarity); (b) alternative view of **2**·1.5CH₂Cl₂ showing the plane defined by the phosphorus and chloride donor atoms, as well as the position of the gold(I) center with respect to this plane.

Table 2. Hydrogen bonds in the crystal structures of **1** and **2**·1.5CH₂Cl₂.



	Contact	1	2·1.5CH ₂ Cl ₂
Intramolecular N–H···Au	H···Au	2.977(48)	2.8345(1), 3.0316(1)
	N···Au	3.565(6)	3.461(4), 3.620(3)
	N–H···Au	146	132.1, 127.4
Intramolecular N–H···Cl/C–H···O	H···Cl/O		2.635(2), 2.586(2)
	N···Cl/O		3.359(6), 3.325(4)
	N/C–H···Cl/O		142.4(4), 144.8(4)
1D	H···O	2.458(5), 2.409(5)	2.699(6), 2.605(5)
	C···O	3.388(9), 3.278(7)	3.468(12), 3.524(6)
	C–H···O	179.1(5), 155.6(4)	140.6(7), 169.5(5)
2D	H···Cl/O	2.842(2)	2.569(7)
	C···Cl/O	3.524(7)	3.429(14)
	C–H···Cl/O	131.1(4)	154.0(7)
3D	H···Cl		2.973(2)
	C···Cl		3.646(5)
	C–H···Cl		130.6(5)

View Article Online
DOI: 10.1039/D6NJ00558F

To eliminate any competitor of the amidic proton (particularly that from the chloride ligand) for the N(amide)-H···Au interaction within a neutral gold(I) complex, compound **2** was treated with 1 equiv. of NaH in anhydrous THF, with the aim of deprotonating one amide group, thus forming an amidate anion, and simultaneously removing the chloride ligand. The reaction afforded a white solid formulated as [Au(L_{-H})] (**3**), exhibiting limited stability, and solubility properties comparable to those of **1** and **2**. Its molar conductivity in acetone solutions (5 × 10⁻⁴ M) was measured as 3.0 Ω⁻¹·cm²·mol⁻¹, confirming its neutral character. Furthermore, compound **3** exhibits spectroscopic features (Figures S9–S12) similar to those of **1** and **2**, including IR bands at 3196–2927 cm⁻¹ [ν(N–H)], and a ³¹P{¹H} NMR singlet at 32.98 ppm. Its ESI(+) mass spectrum shows the molecular ion peak at *m/z* 882.17, also found in the spectra of **1** and **2**. However, in compound **3**, the ¹H NMR signal corresponding to the single NH proton of the amide group, which would be expected for a neutral complex, could not be detected.

An X-ray diffraction analysis was therefore carried out on single crystals obtained by slow diffusion of *n*-hexane into a saturated CH₂Cl₂ solution of the white solid. Due to the relative instability of the compound and quality of the crystals, data collection had to be limited. Despite this limitation, the data still allow us to understand the nature of the compound, which is consistent with the expectations of the synthetic strategy. Although bond lengths and angles could not be determined with sufficient accuracy, the ligation at the metal centre can nevertheless be described, providing a proof of concept. The gold(I) centre is linearly coordinated to the two phosphorus atoms from the ligand **L** (Figure 3) with Au–P distances of about 2.3 Å. The asymmetric Au–N distances (of about 2.9 and 3.4 Å) facilitated the localization of the amide hydrogen atom, which participates in an intramolecular N(amide)-H···Au interaction (H···Au = 2.6 Å, N···Au = 3.4 Å; N–H···Au = 140°), while the deprotonated nitrogen atom, with an Au–N distance of about only 2.9 Å, establishes an unprecedented N(amidate)···Au bonding interaction ([Σ_{vdw}(N, Au) = 3.22 Å].²⁵ Therefore, the removal of the chloride ligand from the coordination sphere of gold(I) upon reaction of **2** with

NaH seems to result in the strengthening of the N(amide)-H···Au interaction, concomitant with the formation of a peculiar intramolecular N(amidate)···Au bonding interaction. RCO(R')N(amidate)–Au bonds are well known in the gold(I) coordination chemistry.^{31–34} In all cases, the amidate anion plays a direct role in defining the linear coordination environment at the metal, exhibiting significantly shorter N–Au bond distances of around 2.0 Å. In **3**, N(amidate)···Au and N(amide)-H···Au interactions, although significantly shorter than the sum of van der Waals radii, act as secondary interactions at the metal centre, whose coordination environment is primarily defined by the two phosphine donors.

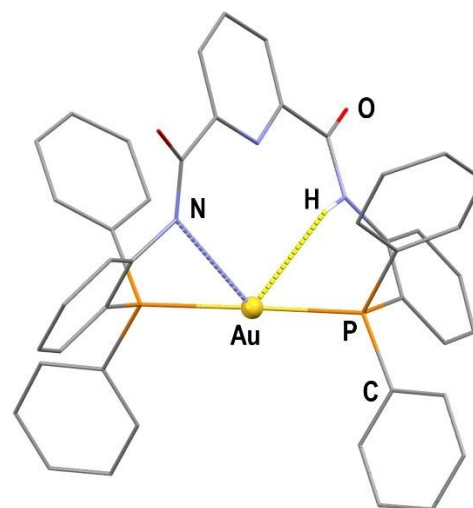


Figure 3. Ligation at the gold(I) centre in Au(L_{-H})] (**3**).

Hirshfeld surface analysis was performed to elucidate the dominant intermolecular interactions governing the crystal packing of complexes **1** and **2**. In both structures (see Figure 4), the *d*_{norm} mapped surfaces display well defined red spots associated with C–H···O hydrogen bonds, confirming that these contacts represent a common and significant stabilizing motif across the series. The

Open Access Article. Published on 23 April 2016. Downloaded on 4/23/2016 12:46:33 PM. This article is licensed under a Creative Commons Attribution 3.0 Unported Licence.



reciprocal nature of these interactions is evident from the characteristic pair of sharp spikes observed in the corresponding 2D fingerprint plots, consistent with moderately strong C–H...O approaches. Complexes **1** and **2** also exhibit C–H...Cl contacts, although their manifestation on the Hirshfeld surface differs between the two systems. In complex **2**, a faint but discernible red region appears near the chloride atom, in line with the presence of short H...Cl approaches. In contrast, complex **1** structure displays intermolecular Cl...H distances below the sum of van der Waals radii, yet these interactions do not generate a red region on the d_{norm} surface, indicating that although geometrically short enough, they are less directional and weaker than those involving oxygen.

Computational studies.

To support the structural evidence of a N(amide)–H...Au hydrogen bond in **2** and **3**, we turned to analyse the electron density in these complexes performing non-covalent interaction (NCI) analysis of the electron density.³⁵ Model systems **2a** and **3a** were initially built up from the corresponding experimental X-ray structures, and fully optimized at DFT PBE(D3)/def2TZVP level of theory,^{36,37} including the empirical dispersion correction described by Grimme.³⁸

The optimized geometrical parameters of **2a** and **3a** are very similar to those observed experimentally (Table S3) including different P–Au–P angles that depend on the gold(I) coordination environment, i.e., three-coordinate and distorted trigonal planar in the case of **2a** and nearly linear and two-coordinate in the case of **3a**. In the case of model **2a** two short NH...Cl stabilizing interactions are optimized, together with longer NH...Au and CH...Au contacts.

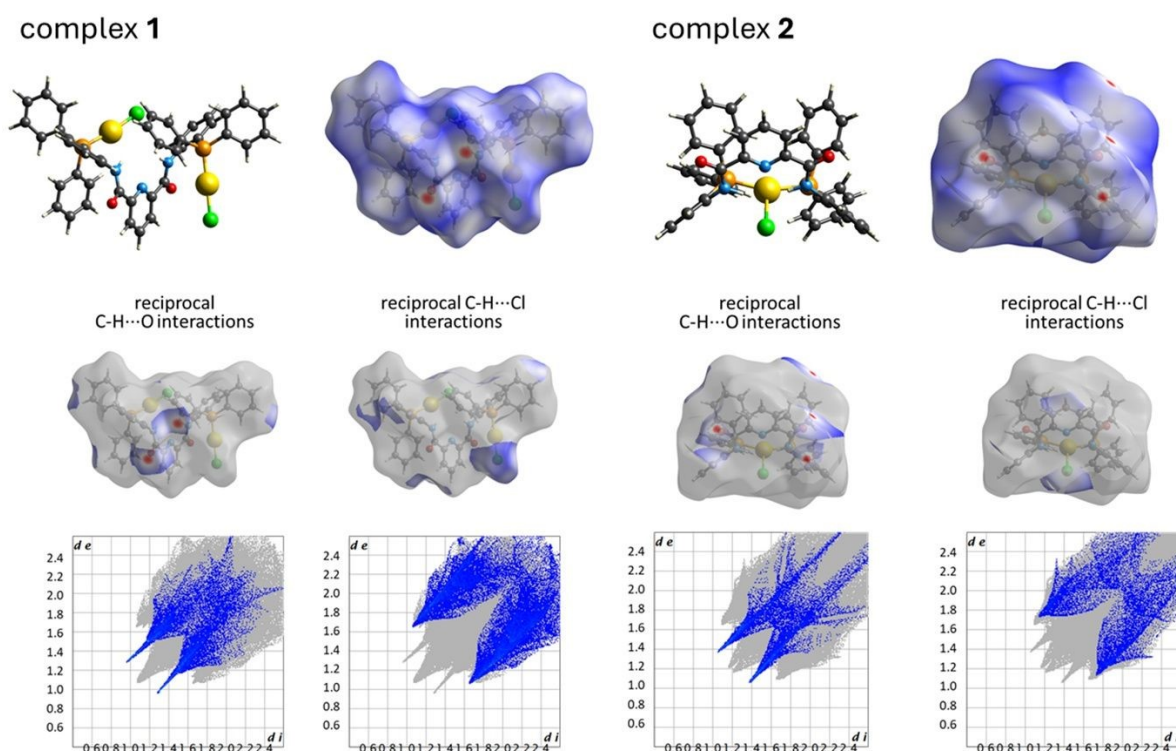


Figure 4. Hirshfeld surface analyses (d_{norm}) and associated 2D fingerprint plots for complexes **1** and **2**, highlighting the main intermolecular interactions.

In the case of the asymmetric model **3a** a markedly shorter NH...Au interaction is optimized at 2.66 Å, which is reinforced by the N(amide)–Au bonding interaction optimized at 2.99 Å, and several CH...Au contacts. These interactions were confirmed by NCI calculations and computation of the intrinsic bond strength index for weak interactions (IBSIW), that provide a relative comparison of the strength of stabilizing intramolecular interactions.

Figures 4 and 5 depict the NCI isosurfaces for the two model systems, showing the spatial distribution of the non-covalent interaction densities in real space as coloured regions. The type of NCI can be determined semi-quantitatively by mapping the electron density multiplied by the sign of the second Hessian eigenvalue, $\text{sign}(\lambda_2)\rho$, onto the iso-surfaces of the reduced

density gradient $\sigma(r)$. When the sign of the second Hessian eigenvalue is positive ($\lambda_2 > 0$), red iso-surfaces appear corresponding to steric and repulsive contacts. When the sign of the second Hessian eigenvalue is close to zero ($\lambda \approx 0$), green iso-surfaces indicate van der Waals weak interactions. Conversely, when the sign of the second Hessian eigenvalue is negative ($\lambda_2 < 0$), green-blue or blue iso-surfaces represent attractive NCIs. In the case of model **2a** the strongest NCIs appear as bluish circles between the NH groups and the Cl atom.



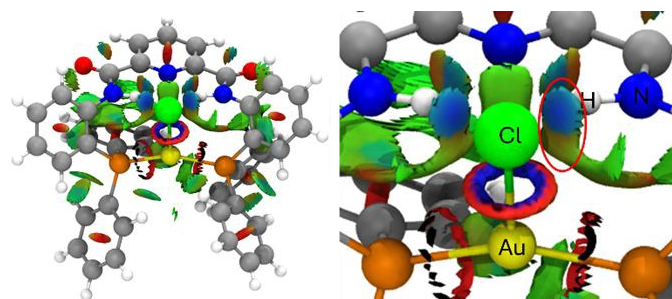


Figure 5. NCI isosurface (isovalue = 0.5 a.u.) of the optimized model system **2a** (left) and detailed isosurface around the gold centre (left) showing the attractive nature of the N-H...Cl and N-H...Au interactions (red circle).

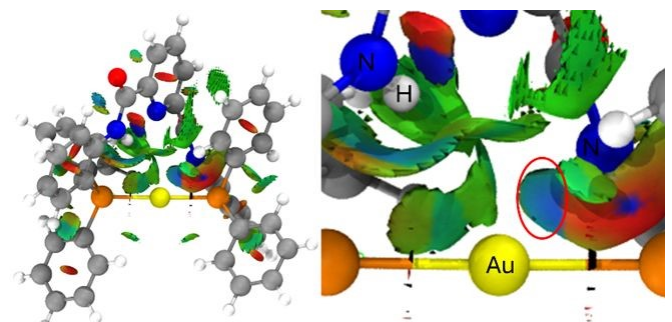


Figure 6. NCI isosurface (isovalue = 0.5 a.u.) of the optimized model system **3a** (left) and detailed isosurface around the gold centre (left) showing the attractive nature of the N(amidate)...Au interaction (red circle).

In addition, below the bluish circles the isosurface is extended as greenish regions indicating the presence of the expected N-H...Au interactions. In addition, other weak van der Waals interactions between C-H groups of the phenyl rings also provide additional stabilizing interactions. In the case of model system **3a**, the strongest NCI is again depicted as a bluish region and represents the N(amidate)...Au interaction. Green regions representing N-H...Au and C-H...Au van der Waals interactions are also displayed. The computed IBSIW indexes (Table S4) confirm that the N(amide)-H...Cl and N(amidate)...Au interactions are attractive NCIs and represent the strongest ones in **2a** and **3a**, respectively. These are followed by the N(amide)-H...Au interaction(s) that are stronger in **3a** than in **2a**, as also inferred from the structural data.

Experimental

N,N'-bis{(2-diphenylphosphanyl)phenyl}-2,6-pyridinedicarboxamide (**L**)^{23,24} and [AuCl(tht)] (CAS 39929-21-0) were prepared following the procedures reported in the literature. All reactions were conducted under a dry N₂ atmosphere, employing standard Schlenk techniques. Solvents were procured from a solvent purification system (M-BRAUN MB SPS-800). Conductivity measurements were performed using a Jenway 4510 digital instrument (Jenway, Felsted, UK). Mass spectrometry data were acquired on a time-of-flight mass spectrometer equipped with an electrospray ionization (ESI) source (Bruker MicroTOF-Q spectrometer, Bruker Corporation, Bremen, Germany). The UATR-IR infrared spectra have been recorded on a Perkin-Elmer 2 spectrophotometer equipped with a diamond crystal UATR attachment, covering a range of 4000–500 cm⁻¹. ³¹P{¹H}- and

¹H-NMR experiments were conducted on a Bruker AVANCE 400 spectrophotometer (Bruker Corporation, Fällanden, Switzerland) in CDCl₃ solutions. Chemical shifts are reported ppm and referenced to H₃PO₄ (³¹P, external) and SiMe₄ (¹H, external). Multiplicities are denoted as singlet (s), triplet (t) or multiplet (m).

Synthesis of [(L)(AuCl)₂] (1) and [(L)AuCl] (2). To a solution of **L** (0.1371 g, 0.2 mmol) in 20 mL of CH₂Cl₂ under an inert atmosphere, [AuCl(tht)] was added [0.1282 g (0.4 mmol) for the synthesis of **1**; 0.0641 g (0.2 mmol) for the synthesis of **2**]. The reaction mixture was stirred at room temperature for 6 hours. After this time, the solvent was partially evaporated under reduced pressure, and the addition of 20 mL of *n*-hexane induced the precipitation of a white solid. The resulting compound was collected by filtration, washed with *n*-hexane (3 × 1 mL), and dried under vacuum (97 % yield for **1**; 48% yield for **2**). Crystals of **1** and **2**·1.5CH₂Cl₂ suitable for X-ray diffraction analysis were obtained by slow diffusion of *n*-hexane into a saturated CH₂Cl₂ solution of the compound at room temperature.

[(L)(AuCl)₂] (1). ¹H-NMR (CDCl₃, 298K), δ_H: 9.36 (s, 2H, H₁, NH), 8.07 (d, 2H, H₂, J = 7.48 Hz), 7.85 (t, 1H, H₃, J = 7.57 Hz), 7.71 (m, 2H, H₄), 7.55–7.38 (m, 14H, H₅, H₉, H₁₀), 7.33–7.31 ppm (m, 10H, H₆, H₈), 6.94–6.87 ppm (m, 2H, H₇) (see Figure S7). ³¹P{¹H}-NMR (CDCl₃, 298K), δ_P: 23.98 ppm (s, PPh₂). UATR-IR: 3017–2946 (m, NH), 1739 (vs, br, CO) 1685 (vs, br, C-Hpy) cm⁻¹. ESI(+): m/z (%): 1114.1125 (55) [C₄₃H₃₃Au₂ClN₃O₂P₂] ([M–Cl]⁺), 882.1760 (30) [C₄₃H₃₃AuN₃O₂P₂] ([M–Au–2Cl]⁺), 375.17 (100) [C₁₉H₁₁N₃O₂P₂] ([L-4Ph2-2H]⁺). Λ_M (acetone, 5 × 10⁻⁴ M): 4.1 Ω⁻¹ cm² mol⁻¹.

[(L)AuCl] (2). ¹H-NMR (CDCl₃, 298K), δ_H: 11.79 (s, 2H, H₁, NH), 8.10 (d, 2H, H₂, J = 7.5 Hz), 7.83 (t, 1H, H₃, J = 7.4 Hz), 7.74 (m, 2H, H₄), 7.54–7.39 (m, 14H, H₅, H₉, H₁₀), 7.33–7.28 ppm (m, 10H, H₆, H₈), 6.91–6.85 ppm (m, 2H, H₇) (see Figure S8). ³¹P{¹H}-NMR (CDCl₃, 298K), δ_P: 34.97 ppm (s, PPh₂). UATR-IR: 3201–3055 (m, NH), 1738 (m, CO), 1682 (vs, br, C-Hpy) cm⁻¹. ESI(+): m/z (%): 882.17 (100) [C₄₃H₃₃Au N₃O₂P₂]⁺ ([M–Cl]⁺). ESI(-): m/z (%): 915.92 (100) [C₄₃H₃₂AuClN₃O₂P₂]⁻ ([M–H]⁻). Λ_M (acetone, 5 × 10⁻⁴ M): 3.2 Ω⁻¹ cm² mol⁻¹.

Synthesis of [Au(L-H)] (3). To a solution of **L** (0.1377 g, 0.15 mmol) in anhydrous THF (10 mL) under an inert atmosphere, sodium hydride (NaH, CAS 7646-69-7, 6.0 mg, 0.25 mmol, 1.1 equivalents) was added. The resulting suspension was stirred at room temperature for 24 h, during which a cloudy, opaque solution formed. The reaction mixture was then filtered through a nylon syringe filter (0.45 μm, Ø 25 mm) to remove any traces of unreacted NaH and the byproduct NaCl. The resulting filtrate was transferred to a second reaction flask under an inert atmosphere and dried under vacuum to afford the new complex as a white solid (42 % yield). ¹H-NMR (CDCl₃, 298K), δ_H: 8.48 (brd, 2H, H₄), 8.07 (d, 2H, H₂, J = 7.5 Hz), 7.65 (t, 1H, H₃, J = 7.54 Hz), 7.62–7.48 (m, 14H, H₅, H₉, H₁₀), 7.39–7.31 (m, 10H, H₆, H₈), 7.04–6.77 (m, 2H, H₇) (see Figure S12). ³¹P{¹H}-NMR (CDCl₃, 298K), δ_P: 32.98 ppm (s, PPh₂). UATR-IR: 3196–2927 (m, NH), 1738 (vs, br, CO), 1684 (vs, br, C-Hpy) cm⁻¹. ESI(+): m/z (%): 882.17 (100)



[C₄₃H₃₃AuN₃O₂P₂]⁺ ([M]⁺). Λ_M (acetone, 5 × 10⁻⁴ M): 3.0 Ω⁻¹ cm² mol⁻¹.

View Article Online
DOI: 10.1039/D6NJ00558F

Table 3. Data collection and structure refinement details for **1** and **2**·1.5CH₂Cl₂.

	1	2 ·1.5CH ₂ Cl ₂
Chemical Formula	C ₄₃ H ₃₃ Au ₂ Cl ₂ N ₃ O ₂ P ₂	C ₄₃ H ₃₃ AuClN ₃ O ₂ P ₂ ·1.5CH ₂ Cl ₂
Crystal habit	colourless	colourless
Crystal size/mm	0.197 × 0.127 × 0.075	0.104 × 0.095 × 0.064
Crystal system	triclinic	monoclinic
Space group	P-1	P2 ₁ /c
a/Å	11.1966(4)	13.6230(5)
b/Å	11.5477(4)	13.1182(5)
c/Å	16.5303(5)	25.1130(10)
α/°	90.624(1)	90
β/°	94.721(1)	99.3630(10)
γ/°	106.150(1)	90
V/Å³	2044.70(12)	4428.1(3)
Z	2	4
D_c/g cm⁻³	1.869	1.377
M	1150.49	918.127
F(000)	1096.1	1812.9
T/°C	23(2)	25(2)
2θ_{max}/°	49.42	55.88
μ(Mo-Kα)/mm⁻¹	7.416	3.502
No. refl. Measured	51359	101847
No. unique refl.	6971	10570
R_{int}	0.0321	0.0629
R[F > 2σ(F)][a]	0.0205	0.0395
wR[F₂, all refl.][b]	0.0443	0.1000
No. of refl. Used [F > 2σ(F)]	6971	10570
No. of parameters	545	488
No. of restraints	0	103
S [c]	1.045	0.998
Max. residual electron density/e·Å⁻³	0.39	0.75

^a $R: (F) = \sum |F_o| - |F_c| / \sum |F_o|$.

^b $wR: (F^2) = [\sum \{w(F_o^2 - F_c^2)^2\} / \sum \{w(F_o^2)^2\}]^{0.5}$; $w^{-1} = \sigma^2(F_o^2) + (aP)^2 + bP$, where $P = [F_o^2 + 2F_c^2]/3$ and a and b are constants adjusted by the program.

^c $S = [\sum \{w(F_o^2 - F_c^2)^2\} / (n-p)]^{0.5}$, where n is the number of data and p the number of parameters.

Computational details. The model systems of complexes **2** and **3** (**2a** and **3a**, respectively) used in the computational studies were built-up based on the X-ray diffraction results and fully optimized at the Density Functional Theory (DFT) level employing the PBE functional,^{36,37} along with the corresponding dispersion correction of Grimme,³⁸ as implemented in TURBOMOLE 6.4.³⁹ A topological analysis of non-covalent interactions (NCI) and IBSIW indexes for each model was conducted using the Multiwfn software.⁴⁰ The electron density representations were generated using the VMD software for visualizing the results.⁴¹

Crystallography.

Suitable single crystals were mounted in inert oil on a MiteGen MicroMount and transferred to the cold nitrogen stream of a Bruker APEX-II CCD area-detector diffractometer, equipped with an Oxford Instruments low-temperature controller system (Mo Kα=0.71073 Å, graphite monochromator). Data were collected in ω- and φ-scan modes. Absorption effects were treated by numerical corrections.

Complex **2** crystallizes with one and a half molecule of solvent per molecule of compound. The structures was solved with the XT structure solution program using intrinsic phasing and refined on F_o² with SHELXL-97.⁴² All non-hydrogen atoms were treated anisotropically, and all hydrogen atoms were included as riding bodies except the amidic hydrogens in **1**, which were located in the Fourier map and refined freely. CCDC 2525580 and 2525581 contain the supplementary crystallographic data for this paper. Hirshfeld isosurfaces and the corresponding fingerprint plots were generated using CrystalExplorer 21.⁴³

Conclusions

This study provides new insights into the nature of weak NH...Au(I) interactions, a topic that remains under debate. Through the synthesis and characterization of a new series of gold(I) complexes with the pincer ligand *N,N'*-bis{(2-diphenylphosphanyl)phenyl}-2,6-pyridinedicarboxamide (**L**), it has been possible to explore the formation of rare examples of



N(amide)H...Au(I) interactions in different coordination environments. In particular, in the neutral compound [Au(L_H)] (**3**), beside an N(amide)H...Au(I) interaction exhibiting clear directionality and structural features consistent with a metal-centered hydrogen bond, an unprecedented secondary N(amidate)...Au weak interaction, is also observed, providing a valuable indication for further structural and computational investigations.

Author contributions

All authors contributed to the writing of the manuscript and approved its final version. The experimental work was conducted by L. C.-G., S. M., J. M. L.-L., M. E. O., C. C., G. P. and V. L., whereas the computational studies were performed by M. M.

Conflicts of interest

There are no conflicts to declare.

Data availability

The data supporting this article have been included as part of the electronic supplementary information (ESI). Supplementary information: spectroscopic characterization, structural characterization and computational studies. See DOI: 10.1039/x0xx00000x

CCDC 2525580 and 2525581 contain the supplementary crystallographic data for this paper.

Acknowledgements

We gratefully acknowledge the DGI MICINN/FEDER (project number PID2022-139739NB-I00 (AEI/FEDER, UE)) and by "ERDF A way of making Europe". L. C.-G. the University of La Rioja for her predoctoral grant. We thank the Università degli Studi di Cagliari for financial support and CeSAR (Centro Servizi d'Ateneo per la Ricerca) of the University of Cagliari.

Notes and references

- 1 Definition of the hydrogen bond (IUPAC Recommendations 2011), E. Arunan, G. R. Desiraju, R. A. Klein, J. Sadlej, S. Scheiner, I. Alkorta, D. C. Clary, R. H. Crabtree, J. J. Dannenberg, P. Hobza, H. G. Kjaergaard, A. C. Legon, B. Mennucci, D. J. Nesbitt, *Pure Appl. Chem.*, 2011, **83**, 1637–1641.
- 2 Definition of the halogen bond (IUPAC Recommendations 2013), G. R. Desiraju, P. S. Ho, L. Kloo, A. C. Legon, R. Marquardt, Pi. Metrangolo, P. Politzer, G. Resnati, Kari Rissanen, *Pure Appl. Chem.*, 2013, **85**, 1711–1713.
- 3 Definition of the Chalcogen bond (IUPAC Recommendations 2019), C. B. Aakeroy, D. L. Bryce, G. R. Desiraju, A. Frontera, A. C. Legon, F. Nicotra, K. Rissanen, S. Scheiner, G. Terraneo, P. Metrangolo, G. Resnati, *Pure Appl. Chem.*, 2019, **91**, 1889–1892.
- 4 *Supramolecular Chemistry*, J. W. Steed, J. L. Atwood (Eds.), Wiley, 2009, ISBN: 9780470512333, DOI: 10.1002/9780470740880.

- 5 A comprehensive review of the spodium bond as a new crystal engineering motif in Zn/Cd complexes: challenges and future perspectives, S. Hazra, D. Majumdar, D. Das, L. Barman, S. Roy, S. Dalai, *Dalton Trans.*, 2026, **55**, 1584–1624.
- 6 Agostic interactions in transition metal compounds, M. Brookhart, M. L. H. Green, G. Parkin, *Proc. Natl. Acad. Sci. USA*, 2007, **104**, 6908–6914.
- 7 Metals and hydrogen bonds, L. Brammer, *Dalton Trans.*, 2003, 3145–3157.
- 8 Hydrogen bonds involving transition metal centers acting as proton acceptors, A. Martín, *J. Chem. Educ.*, 1999, **76**, 578–583.
- 9 Gold-Catalyzed Organic Reactions, A. S. K. Hashmi, *Chem. Rev.*, 2007, **107**, 3180–3211.
- 10 Gold-catalyzed cycloisomerizations of enynes: a mechanistic perspective, E. Jiménez-Nuñez, A. M. Echavarren, *Chem. Rev.*, 2008, **108**, 3326–3350.
- 11 Optimizing catalyst and reaction conditions in gold(I) catalysis–ligand development, A. Collado, D. J. Nelso, S. P. Nolan, *Chem. Rev.*, 2021, **121**, 8559–8612.
- 12 The gold-hydrogen bond, Au–H, and the hydrogen bond to gold, Au...H–X, H. Schmidbaur, H. G. Raubenheimer, L. Dobrzańska, *Chem. Soc. Rev.*, 2014, **43**, 345–380.
- 13 Proof of Concept for Hydrogen Bonding to Gold, Au...H–X, H. Schmidbaur, *Angew. Chem. Int. Ed.*, 2019, **58**, 5806–5809.
- 14 Deciphering the Primary Role of Au...H–X Hydrogen Bonding in Gold Catalysis, A. Sorroche, S. Moreno, M. El. Olmos, M. Monge, J. M. López-de-Luzuriaga, *Angew. Chem. Int. Ed.*, 2023, **62**, e202310314 (1–9).
- 15 [Rb([18]crown-6)(NH₃)₃]Au·NH₃: Gold as Acceptor in N–H...Au[–] Hydrogen Bonds, H. Nuss, M. Jansen, *Angew. Chem. Int. Ed.*, 2006, **45**, 4369–4371.
- 16 Hydride Transfer to Gold: Yes or No? Exploring the Unexpected Versatility of Au...H–M Bonding in Heterobimetallic Dihydrides, L. Rocchigiani, W. T. Looster, S. J. Coles, D. L. Hughes, P. Hrobárik, M. Bochmann, *Chem. Eur. J.*, 2020, **26**, 8267–8280.
- 17 Spectroscopic and Computational Evidence of Intramolecular Au¹⁺...H⁺–N Hydrogen Bonding, M. Straka, E. Andris, J. Vícha, A. Růžička, J. Roithová L. Rulíšek, *Angew. Chem. Int. Ed.*, 2019, **58**, 2011–2016.
- 18 Evidence for genuine hydrogen bonding in gold(I) complexes, M. Rigoulet, S. Massou, E. D. Sosa Carrizo, S. Mallet-Ladeira, A. Amgoune, K. Miqueu, D. Bourissou, *Proc. Natl. Acad. Sci. USA*, 2019, **116**, 46–51.
- 19 Preparing Gold(I) for Interactions with Proton Donors: The Elusive [Au]...HO Hydrogen Bond, F. Groenewald F, J. Dillen, H. G. Raubenheimer, C. Esterhuysen, *Angew. Chem. Int. Ed. Engl.*, 2016, **55**, 1694–1698.
- 20 Hydrogen bonds to Au in coordinated gold clusters, M. A. Bakar, M. Sugiuchi, M. Iwasaki, Y. Shichibu, K. Konishi *Nat. Commun.*, 2017, **8**:576, 1–7.
- 21 A Relativity Enhanced, Medium-Strong Au(I)...H–N Hydrogen Bond in a Protonated Phenylpyridine-Gold(I) Thiolate R. J. F. Berger, J. Schoiber, U. Monkowius, *Inorg. Chem.*, 2017, **56**, 956–961.
- 22 Gold(I) complexes of 2-(diphenylphosphino)aniline: synthesis and influence of the perhalophenyl ligand on their assembly, L. Coconubo-Guio, S. Moreno, M. Monge, M. E. Olmos, José M. Lopéz-de-Luzuriaga, *Dalton Trans.*, 2025, **54**, 15923–15932
- 23 New Palladium, platinum and nickel complexes based on rigid phosphorus and nitrogen ligands, E. K. van den Beuken, A. Meetsma, H. Kooijman, A. L. Spek, B. L. Feringa, *Inorg. Chim. Acta*, 1997, **264**, 171–183.
- 24 Multiple-Functional Diphosphines: Synthesis, Characterization, and Application to Pd-Catalyzed Alkoxycarbonylation of Alkyne, K.-C. Zhao, L. Liu, X.-C. Chen,



- 1
2
3
4
5
6
7
8
9
10
11
12
13
14
15
16
17
18
19
20
21
22
23
24
25
26
27
28
29
30
31
32
33
34
35
36
37
38
39
40
41
42
43
44
45
46
47
48
49
50
51
52
53
54
55
56
57
58
59
60
- Y.-Q. Yao, L. Guo, Y. Lu, X.-L. Zhao, Y. Liu, *Organom.*, 2022, 41, 750–760.
- 25 Van der Waals Volumi and Radii, A. Bondi, *J. Phys. Chem.*, 1964, 68, 441–451.
- 26 Lewis-base adducts of Group 11 metal(I) compounds. Part 27. Solid-state phosphorus-31 cross-polarization magic-angle spinning nuclear magnetic resonance, far-infrared, and structural studies on the mononuclear 2:1 adducts of triphenylphosphine with copper(I) and gold(I) halides, G. A. Bowmaker, J. C. Dyason, P. C. Healy, L. M. Engelhardt, C. Pakawatchai and A. H. White, *J. Chem. Soc., Dalton Trans.*, 1987, 1089.
- 27 Polymorphic Crystal Approach to Changing the Emission of [AuCl(PPh₃)₂], Analyzed by Direct Observation of the Photoexcited Structures by X-ray Photocrystallography, M. Hoshino, H. Uekusa, S. Ishii, T. Otsuka, Y. Kaizu, Y. Ozawa and K. Toriumi, *Inorg. Chem.*, 2010, 49, 7257–7265.
- 28 Gold(I) Hydride Intermediate in Catalysis: Dehydrogenative Alcohol Silylation Catalyzed by Gold(I) Complex, H. Ito, T. Saito, T. Miyahara, C. Zhong and M. Sawamura, *Organom.*, 2009, 28, 4829–4840.
- 29 Selective Lithiation and Phosphane-Functionalization of [(η⁷-C₇H₇)Ti(η⁵-C₅H₅)] (Troticene) and Its Use for the Preparation of Early-Late Heterobimetallic Complexes, S. K. Mohapatra, S. Büschel, C. Daniliuc, P. G. Jones and M. Tamm, *J. Am. Chem. Soc.*, 2009, 131, 17014–17023.
- 30 Di- and Trinuclear Gold Complexes of Diphenylphosphinoethyl-Functionalised Imidazolium Salts and their N-Heterocyclic Carbenes: Synthesis and Photophysical Properties, S. Bestgen, M. T. Gamer, S. Lebedkin, M. M. Kappes and P. W. Roesky, *Chem. Eur. J.*, 2015, 21, 601–614.
- 31 [{Au(IPr)}₂(μ-OH)]X Complexes: Synthetic, Structural and Catalytic Studies, R. S. Ramon, S. Gaillard, A. Poater, L. Cavallo, A. M. Z. Slawin, S. P. Nolan, *Chem. Eur. J.*, 2011, 17, 1238–1246.
- 32 Synthesis and further reactivity studies of some transition metal gallyl complexes, C. Jones, D. P. Mills, R. P. Rose, A. Stasch, W. D. Woodul, *J. Organom. Chem.*, 2010, 695, 2410–2417.
- 33 Gold-containing derivatives of cyclopropanecarboxylic acid amides, E.G. Perevalova, I. G. Bolesov, Ye. S. Kalyuzhnaya, T. I. Voyevodskaya, L. G. Kuzmina, V. I. Korsunsky, K. I. Grandberg, *J. Organom. Chem.*, 1989, 369, 267–280.
- 34 Mono and dinuclear gold(I) complexes with neutral and deprotonated 1,4-benzodiazepin-2-ones. Crystal and molecular structure of (L-H)Au(PPh₃)·Et₂O, where L = 1,3-dihydro-7-nitro-5-phenyl-2H-1,4-benzodiazepin-2-one, nitrazepam, M. A. Cinellu, S. Stoccoro, G. Minghetti, A. L. Bandini, F. Demartin, *Inorg. Chim. Acta*, 1990, 168, 33–41.
- 35 Revealing Noncovalent Interactions, E.R. Johnson, S. Keinan, P. Mori-Sánchez, J. Contreras-García, A.J. Cohen, W. Yang, *J. Am. Chem. Soc.*, 2010, 132, 6498–6506.
- 36 R.G. Parr, W. Yang, *Density-Functional Theory of Atoms and Molecules*; Oxford University Press: New York, NY, USA, 1989.
- 37 Development of the Colle-Salvetti correlation-energy formula into a functional of the electron density, C. Lee, W. Yang, R.G. Parr, *Phys. Rev. B*, 1988, 37, 785–789.
- 38 A consistent and accurate *ab initio* parametrization of density functional dispersion correction (DFT-D) for the 94 elements H-Pu, S. Grimme, J. Antony, S. Ehrlich, H. Krieg, *J. Chem. Phys.*, 2010, 132, 154104.
- 39 Electronic structure calculations on workstation computers: The program system turbomole, R. Ahlrichs, M. Bär, M. Häser, H. Horn, C. Kölmel, *Chem. Phys. Lett.*, 1989, 162, 165–169.
- 40 Multiwfn: A multifunctional wavefunction analyzer, T. Lu, F. Chen, *J. Comput. Chem.*, 2012, 33, 580–592.
- 41 VMD: visual molecular dynamics, W. Humphrey, A. Dalke, K. Schulten, *J. Mol. Graph.*, 1996, 14, 33–38.
- 42 G. M. Sheldrick SHELXL-97, Program for Crystal Structure Refinement, University of Göttingen, Göttingen, Germany, 1997.
- 43 P. R. Spackman, M. J. Turner, J. J. McKinnon, S. K. Wolff, D. J. Grimwood, D. Jayatilaka, M. A. Spackman, *J. Appl. Cryst.* 2021, 54, 1006–1011.

Downloaded on 04/23/2026 10:46:33 AM
 This article is licensed under a Creative Commons Attribution 3.0 Unported Licence.





**UNIVERSITÀ DEGLI STUDI
DI CAGLIARI**



View Article Online
DOI: 10.1039/D6NJ00558F

HR EXCELLENCE IN RESEARCH

The data underlying this study are available in the published article and its Electronic Supplementary Information.

Claudia Caltagirone

Vito Lippolis

M. Elena Olmos

New Journal of Chemistry Accepted Manuscript

1
2
3
4
5
6
7
8
9
10
11
12
13
14
15
16
17
18
19
20
21
22
23
24
25
26
27
28
29
30
31
32
33
34
35
36
37
38
39
40
41
42
43
44
45
46
47
48
49
50
51
52
53
54
55
56
57
58
59
60

Downloaded from www.rsc.org on 23 April 2023. This article is licensed under a Creative Commons Attribution 3.0 Unported Licence.